

## Dielectric relaxation at the glass transition of confined *N*-methyl- $\epsilon$ -caprolactam

D. Daoukaki

*National Technical University of Athens, Department of Physics, Zografou Campus, GR-15780 Athens, Greece*

G. Barut, R. Pelster, and G. Nimtz

*Universität zu Köln, II. Physikalisches Institut, Zùlpicher strasse 77, 50937 Köln, Germany*

A. Kyritsis and P. Pissis

*National Technical University of Athens, Department of Physics, Zografou Campus, GR-15780 Athens, Greece*

(Received 9 December 1997; revised manuscript received 25 March 1998)

The effects of confinement on the glass transition of the nonassociating glass-forming liquid *N*-methyl- $\epsilon$ -caprolactam were studied in detail by means of broadband dielectric relaxation spectroscopy, 5 Hz–2 GHz, and thermally stimulated depolarization current measurements, 77–300 K. The liquid was two dimensionally confined in the pores of controlled porous glasses with mean pore diameter  $d=2.5, 5.0, 7.5,$  and  $20.0$  nm (Gelsil glasses) and  $d=4.0$  nm (Vycor glass) and three dimensionally confined in butyl rubber with mean droplet diameter  $d=7.6$  nm. The confined liquid is classified into two fractions: a relatively immobile interfacial layer close to the wall and the inner layer (volume liquid). For the volume liquid the  $\alpha$  relaxation associated with the glass transition becomes faster and the glass transition temperature decreases compared to the bulk liquid. These effects increase with decreasing  $d$  and are stronger for three- than for two-dimensional confinement. They can be understood on the basis of the cooperativity concept and the configurational entropy model of Adam and Gibbs. The systematic variation of  $d$  allows the determination of the cooperativity length  $\xi$  at  $T_g$  to  $\xi \leq 10$ – $12$  nm. [S0163-1829(98)06533-3]

### I. INTRODUCTION

In a recent paper<sup>1</sup> dielectric relaxation spectroscopy (DRS) over wide ranges of frequency and temperature was employed to investigate the relaxational behavior of the glass-forming liquid *N*-methyl- $\epsilon$ -caprolactam (NMEC) confined to the mesopores of a controlled porous glass (CPG) with 10.2-nm-pore diameter. Three distinct relaxation peaks were observed: a slow relaxation assigned to a relatively immobile interfacial layer, an intermediate one originating from interfacial Maxwell-Wagner-Sillars (MWS) polarization of the heterogeneous system, and the  $\alpha$  process associated with the glass transition. The  $\alpha$  process was found to become slightly faster for the confined liquid compared to bulk NMEC, resulting in a lowering of the glass transition temperature  $T_g$  by 5 K. In this work we study in detail the dynamics of the glass transition of NMEC in three different confining geometries: two CPG systems, Gelsil glasses with mean pore diameter  $d=2.5, 5.0, 7.5,$  and  $20$  nm and Vycor glass with  $d=4.0$  nm, and butyl rubber (BR) with hydrophilic inclusions. In the CPG the liquid is two dimensionally (2D) confined in the system of interconnected pores, whereas in BR confinement is three dimensional (3D) occurring in droplets. For this study we employ broadband DRS (5 Hz–2 GHz) and thermally stimulated depolarization currents (TSDC) techniques, characterized by high sensitivity and high resolving power.<sup>2,3</sup>

The investigation of the structural and the dynamic properties of liquids confined in mesoscopic volumes has attracted much interest in recent years.<sup>4,5</sup> Controlled porous glasses have been extensively used as model systems for restricted geometries in these studies. However, connections

made between the geometry of the confining space and the molecular behavior are frequently controversial. A main reason for that is the difficulty associated with the separation of true confinement (finite-size) effects from the influence of the pore surface. Other effects that have to be taken into account may include packing effects, changes of the density of the liquid in the pores, surface-induced alignment, and strong anisotropy of molecular motions. These and similar complications may justify objections against implications from confinement studies on bulk properties and, at least, one has to discuss critically such implications. Despite these objections, it is now in generally believed that the structural and the dynamic properties of confined liquids are modified compared to the bulk properties and that confinement studies may contribute to a better understanding of basic phenomena.<sup>4,5</sup> From the methodological point of view we are discussing here, it deserves to be stressed that the selection of a variety of confining geometries [with respect to matrix material, state (modification<sup>4,5</sup>) of the inner surfaces, size of confinement, dimensionality of confinement, etc.] may be of significant importance in separating true confinement from other effects. We will come back to this point later on.

The investigation of confinement effects on the dynamics of the glass transition in glass-forming liquids and polymers is of particular importance. In many theories and models of the glass transition cooperativity effects play a central role.<sup>6,7</sup> In the configurational entropy model of glass formation of Adam and Gibbs,<sup>8</sup> developed for a bulk system, the existence of cooperatively rearranging regions is assumed. The size of these regions (spheres of radius  $\xi$ ) increases with decreasing temperature, until, at a certain temperature  $T_0$ , the cooperative region comprises the whole system, causing the sharp

reduction of mobility observed in the experiments. Size effects on the glass transition, as a direct consequence of cooperativity effects,<sup>9,10</sup> should appear when the confining length becomes smaller than the cooperativity length (characteristic length of the glass transition)  $\xi$ . Thus, the investigation of confinement effects on the dynamics of the glass transition may assist checking theories and models of the glass transition (of which there exists no generally accepted theory). Moreover, the experimental observation of size effects (e.g., in measurements with varying confining length) would yield  $\xi$  most directly.<sup>9</sup>

Differential scanning calorimetry<sup>11,12</sup> (DSC), DRS,<sup>1,10,13–15</sup> TSDC techniques,<sup>10</sup> and solvation dynamics techniques<sup>16,17</sup> have been employed to study confinement effects on the glass transition in glass-forming liquids two dimensionally confined in the pores of CPG. A broadening of the response at  $T_g$ , compared to the bulk response, was observed in all measurements. Whereas DSC and TSDC measurements clearly show a lowering of  $T_g$  of the confined liquids,<sup>10–12</sup> the respective results of DRS measurements are rather controversial, showing shifts of  $T_g$  to both lower and higher temperatures.<sup>1,10,13–15</sup> It has been suggested that the sign and the magnitude of  $\Delta T_g = T_g(\text{bulk}) - T_g(\text{confined})$  is material specific.<sup>1</sup> From theoretical models of the glass transition and computer simulations both positive<sup>18</sup> and negative<sup>9,19</sup> signs of  $\Delta T_g$  have been predicted.

In this work we study the effects on the glass transition of 2D and 3D confinement of the same liquid. In addition, we vary systematically the size of confinement (pore diameter  $d$  of the CPG used). We employ broadband DRS, which allows the measurement, in separated frequency regions, of the dynamics of the interfacial liquid layer and of the volume liquid,<sup>1</sup> and TSDC techniques, which allow the measurement, with high sensitivity and high resolving power, of the dielectric response of the liquid against temperature at cooling and heating rates comparable to those in DSC.<sup>2,3</sup> Bearing in mind the difficulties for a straightforward interpretation of confinement studies in terms of size-induced effects, the strategy was chosen to vary as much as possible the experimental conditions: matrix material, size of confinement, dimensionality of confinement, dielectric technique used. From the methodological point of view there is an analogy to considering several cases and concentrating on the essential aspects of the phenomenon under investigation through the process of abstraction. Thus, we expect that critical discussion of the results of these measurements may enable us, in particular, to separate pure confinement (physical) from interfacial (chemical) effects<sup>4,5,19</sup> (in addition to the possibility of chemical modification of the inner pore wall)<sup>1,11</sup> and to give quantitative estimates of the cooperativity length  $\xi$ .

NMEC studied here is a typical nonassociating low molecular weight glass-forming liquid. In a parallel investigation propylene glycol is being studied, as a representative of H-bonded liquids, and the results will be published in a separate paper.

## II. EXPERIMENT

NMEC, 99.9%, was obtained from Sigma, St. Louis, and used without further treatment.

BR with hydrophilic components, similar to that used in a previous investigation on the properties of dispersed mesoscopic water droplets,<sup>20</sup> was provided by Bayer, AG, Leverkusen. For filling BR with NMEC dry circular samples of 15 mm diameter and 1 mm thickness were placed in a NMEC bath in an autoclave (373 K, 2.3 bars). The weight of the BR samples was recorded as a function of time and it was found that diffusion followed Fickian behavior with maximum liquid uptake 30 vol. %. By this procedure samples with several filling factors  $f$ , defined as liquid volume in the sample divided by sample volume, between 15% and 30% were prepared.<sup>21</sup> Small-angle x-ray-scattering (SAXS) measurements on the sample with  $f=30\%$ , studied in detail by DRS, showed that, similar to water<sup>20</sup> and to propylene glycol<sup>48</sup> (PG) in BR, NMEC is dispersed in droplets with mean droplet diameter  $d=7.6$  nm.

Vycor glass samples (Corning, No. 7930) with mean pore diameter  $d=4.0$  nm were of cylindrical shape with 15 mm diameter and about 1 mm thickness. Gelsil samples (GelTech Inc.), also of cylindrical shape with 10 mm diameter and about 1 mm thickness, have nominal pore diameter 2.5, 5.0, 7.5, and 20 nm. The CPG samples were thoroughly cleaned and dried according to the producers' instructions and filled to saturation by immersion in NMEC. Some of the Vycor glass samples were chemically treated using hexamethyldisilazane<sup>1,11</sup> to convert the surface hydroxyl groups to the less polar trimethylsilyl groups. This treatment makes the glass more hydrophobic.

For broadband DRS measurements two network analyzers, HP 3577B and HP 8510B were used. By means of a calibration technique allowing temperature-dependent calibration,<sup>22</sup> transmission measurements were performed in the frequency range  $\nu=5$  Hz–2 GHz in a single sweep and for temperatures 100–300 K. Calibration standards and samples were placed in a shielded capacitorlike measurement cell. The temperature was controlled to better than 0.1 K measured over the period of a frequency sweep. For the measurements on bulk NMEC a disk sample geometry was used, a Teflon cell with nickel-coated stainless-steel electrodes of 15 mm diameter at a distance of 1 mm from each other.

TSDC measurements, which correspond to measurements of dielectric losses against temperature at fixed frequencies of  $10^{-2}$ – $10^{-4}$  Hz,<sup>2</sup> were carried out in the temperature range 77–300 K, on the same samples used for DRS measurements. The BR and the CPG samples were clamped between brass electrodes. A disk sample geometry was used also for measurements on bulk NMEC with brass electrodes. The method has been described in detail elsewhere.<sup>2,3</sup> Here we recall briefly the TSDC procedure. The sample is polarized by a dc electric field  $E_p$  at temperature  $T_p$  for a time  $t_p$  and its polarization is quenched at a sufficiently low temperature  $T_0$ . By warming the sample at a linear heating rate  $b$  in short-circuit conditions, the polarization decays and the corresponding depolarization current is detected by an electrometer. For each relaxation mechanism an inherent current peak is recorded. The analysis of the shape of the recorded thermogram allows one to obtain the contribution  $\Delta\epsilon$  of a peak to the static permittivity and the thermodynamic and form parameters of the underlying relaxation mechanism.<sup>2,3</sup> For details of the apparatus used we refer to Ref. 3.

We would like to mention here that the experimental

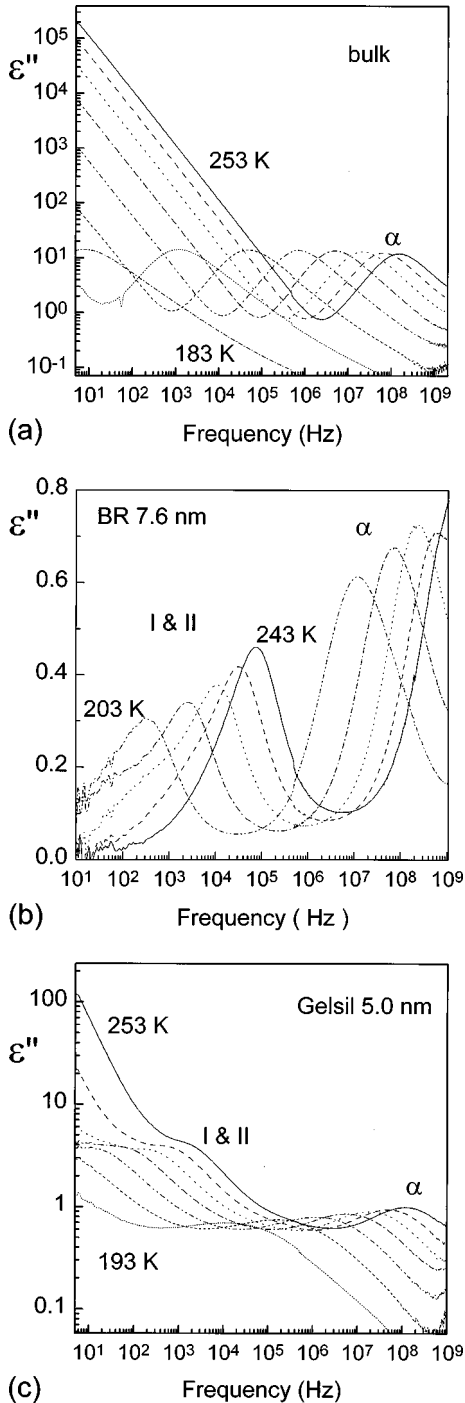


FIG. 1. Dielectric loss  $\epsilon''$  vs frequency  $\nu$  for NMEC bulk (a) and confined in BR (filling factor  $f=30\%$ , mean droplet diameter  $d=7.6$  nm) (b) and in Gelsil glasses with mean pore diameter  $d=5.0$  nm (c) at several temperatures, in steps of 10 K, indicated on the plots.

setup of two parallel atomically smooth plates as used for surface force measurements is from the conceptual point of view the most well-defined one for confined studies. This setup is, however, not possible to realize for temperature-dependent dielectric measurements.

### III. RESULTS

Figures 1(a)–1(c) show in log-log plots the dielectric loss  $\epsilon''$  against frequency  $\nu$  at several selected temperatures for

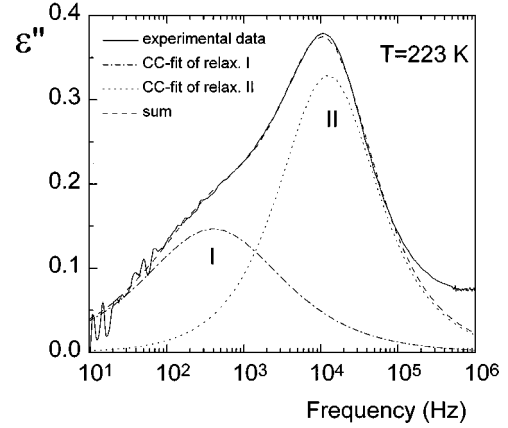


FIG. 2.  $\epsilon''(\nu)$  for NMEC in BR ( $f=30\%$ ,  $d=7.6$  nm) at low frequencies at 223 K and separation by fitting into Rel I and Rel II.

NMEC bulk [Fig. 1(a)] and confined in BR with filling factor  $f=30\%$  and mean droplet diameter  $d=7.6$  nm [Fig. 1(b)] and in Gelsil glasses with mean pore diameter  $d=5.0$  nm [Fig. 1(c)]. In Fig. 1(a) we observe the  $\alpha$  relaxation associated with the glass transition and at low frequencies the sharp increase of  $\epsilon''$  with decreasing  $\nu$  due to dc conductivity. Measurements on dry BR and unfilled CPG samples for comparison show negligible losses (despite a weak  $\alpha$  process in BR with  $T_g$  around 200 K), so that the response in Figs. 1(b) and 1(c) is practically determined by the presence of the liquid. Besides the  $\alpha$  process we observe in Figs. 1(b) and 1(c) a broad complex dispersion at lower frequencies and a conductivity wing for Gelsil (interestingly, however, not for BR).

For a quantitative analysis of the dielectric spectra a superposition of model functions according to Havriliak and Negami<sup>23</sup> and a conductivity contribution have been fitted to  $\epsilon''(\omega)$ ,  $\omega=2\pi\nu$ :

$$\epsilon'' = \frac{\sigma_{dc}}{\epsilon_0 \omega^s} - \sum_{k=1}^3 \text{Im} \left[ \frac{\Delta \epsilon_k}{[1 + (i\omega/\omega_{HNk})^{1-\alpha_k}]^{\gamma_k}} \right]. \quad (1)$$

The first term on the right-hand side of Eq. (1) quantifies the dc conductivity  $\sigma_{dc}$  in terms of  $\epsilon''(\omega)$  with a fit parameter  $s$ ,  $s=1$  for Ohmic conductivity (bulk liquid) and  $s<1$  otherwise.  $\epsilon_0$  is the vacuum permittivity.  $\Delta \epsilon$  is the relaxation strength and  $\omega_{HN}$  the position on the frequency scale of the relaxation process. The index  $k$  refers to the different processes that contribute to the dielectric response. The exponents  $\alpha$  and  $\gamma$  [ $0 < (1-\alpha)$ ,  $(1-\alpha)\gamma \leq 1$ ] define the symmetrical and asymmetrical broadening of the loss peaks, respectively, with respect to the Debye peak [ $(1-\alpha)=\gamma=1$ ]. The loss peak at the highest frequency is due to the  $\alpha$  process and is present in all spectra. The other two peaks, Rel I and Rel II in the order of increasing frequency, present in the confined liquid spectra in the region of the complex broad dispersion, could be satisfactorily fitted by the symmetrical Cole-Cole expression [ $\gamma=1$  in Eq. (1) (Ref. 23)]. An example of this analysis is shown in Fig. 2. In the following section it will be shown that Rel I and Rel II are assigned, in agreement with Ref. 1, to a relatively immobile interfacial layer and to interfacial Maxwell-Wagner-Sillars

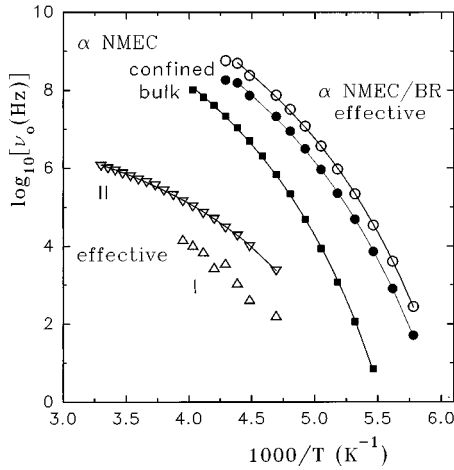


FIG. 3. Arrhenius plot of the peak frequency  $\nu_0$  for NMEC bulk (■) and confined in BR with  $f=30\%$  and  $d=7.6$  nm ( $\alpha$  relaxation, effective values, ○;  $\alpha$  relaxation, corrected effective values, ●; Rel I,  $\rho$ ; Rel II,  $\sigma$ ). The lines are VFT fits to the data.

polarization of the heterogeneous system, respectively. In what follows we focus on the  $\alpha$  process. Information on confinement effects will be obtained from the investigation of modifications induced by confinement on the temperature dependence of the relaxation rate of the  $\alpha$  process (Arrhenius plots) and on the shape of the loss peak.

The dielectric behavior in Figs. 1(b), 1(c), and 2 refers to the composite system matrix plus confined liquid alone. Effective medium theories<sup>24</sup> can be used to calculate the dielectric properties of the confined liquid from the measured (effective) properties of the composite system. The calculation is straightforward for BR as a matrix where the liquid is three dimensionally confined in spherical droplets (SAXS experiments). Because of the rather high filling factor,  $f=30\%$ , the Hanai-Bruggemann formula has been used.<sup>24</sup>

$$\frac{\varepsilon_{\text{eff}} - \varepsilon_p}{\varepsilon_m - \varepsilon_p} \left( \frac{\varepsilon_m}{\varepsilon_{\text{eff}}} \right)^{1/3} = 1 - f. \quad (2)$$

$\varepsilon_{\text{eff}}$ ,  $\varepsilon_m$ , and  $\varepsilon_p$  are the complex dielectric functions of the composite system (the measured one), the matrix (BR) and the liquid, respectively. Using reasonable approximations and the measured values of BR ( $\varepsilon_m$ ), the measured (effective) values have been corrected to receive the corresponding values for the confined liquid. With respect to the  $\alpha$  process we focus on, the correction refers to the position of the loss peak ( $\nu_0$ ), the shape of the response, and the relaxation strength  $\Delta\varepsilon$  (details to be published elsewhere). As a result of the rather high filling factor  $f=30\%$  the corrections are rather small, examples to be given below. The corrections are expected to be significantly smaller for CPG's because of both the shape of the inclusions and the higher filling factors.

Figure 3 shows the Arrhenius plot of the three processes in NMEC confined in BR and of the  $\alpha$  process in the bulk liquid. For the  $\alpha$  process in BR both the uncorrected (measured, effective) and the corrected values of  $\nu_0$  are shown. The temperature dependence of the frequency of loss peak maximum  $\nu_0$  for the  $\alpha$  process, both in the bulk and the confined liquid, and for the MWS process is well described by the Vogel-Fulcher-Tammann (VFT) equation<sup>6,7</sup>

TABLE I. Values of  $\log_{10}A, B, T_0$  (VTF equation), glass transition temperature  $T_g$ , determined by  $\tau(T_g)=100$  s, and  $\Delta T_g = T_g$  (bulk) -  $T_g$  (confined), for NMEC in BR with  $f=30\%$  and  $d=7.6$  nm.

|            | $\log_{10}A$ | $B$ (K) | $T_0$ (K) | $T_g$ (K) | $\Delta T_g$ (K) |
|------------|--------------|---------|-----------|-----------|------------------|
| NMEC bulk  | 12.63        | 481.2   | 142.3     | 173.5     |                  |
| Effective  |              |         |           |           |                  |
| NMEC in BR | 13.43        | 456.7   | 131.5     | 159.6     | 13.9             |
| Corrected  |              |         |           |           |                  |
| NMEC in BR | 13.21        | 488.7   | 130.6     | 161.1     | 12.4             |

$$\nu_0 = A \exp\left(-\frac{B}{T-T_0}\right), \quad (3)$$

where the preexponential factor  $A$ , the activation parameter  $B$ , and the Vogel temperature  $T_0$  are temperature-independent empirical parameters. The glass transition temperature  $T_g$  of bulk and confined NMEC was determined from plots similar to those in Fig. 3 by the condition  $\tau(T_g)=100$  s, where  $\tau$  the dielectric relaxation time,  $\tau=1/(2\pi\nu_0)$ .  $T_g$  may depend on the method of measurement and the definition, the dependence being less pronounced for the shift of  $T_g$ ,  $\Delta T_g = T_g(\text{bulk}) - T_g(\text{confined})$ , which is the quantity of interest here. The values of  $\log_{10}A, B, T_0, T_g$ , and  $\Delta T_g$  are listed in Table I.

TSDC thermograms in the temperature region of the glass transition are shown in Figs. 4 and 5 for NMEC bulk and confined in Vycor and in BR. The peak temperature  $T_m$  is a good measure of  $T_g$ .<sup>3</sup> Figure 6 shows  $\Delta T_g$  determined by DRS and TSDC against nominal size of confinement, i.e., pore/droplet diameter  $d$ .

The results concerning the shape of the response will be rationalized by means of the Havriliak-Negami expression

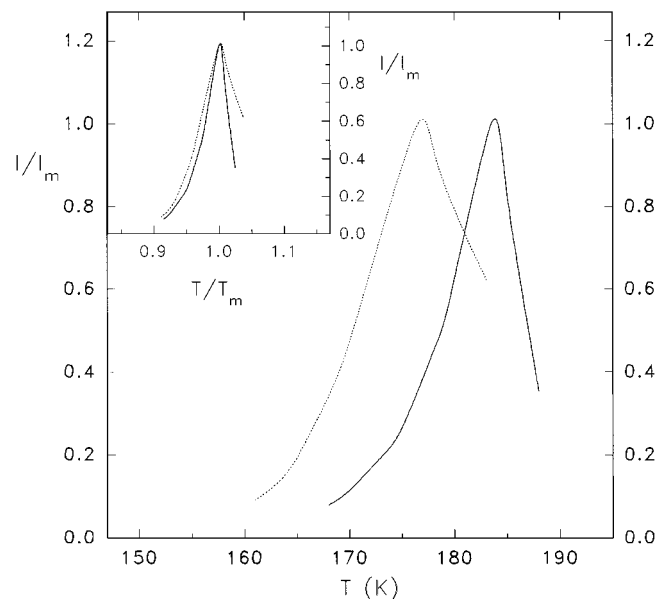


FIG. 4. TSDC thermograms normalized to unit height for NMEC bulk (—) and confined in Vycor glass,  $d=4.0$  nm (---). The inset shows the corresponding scaling plots.

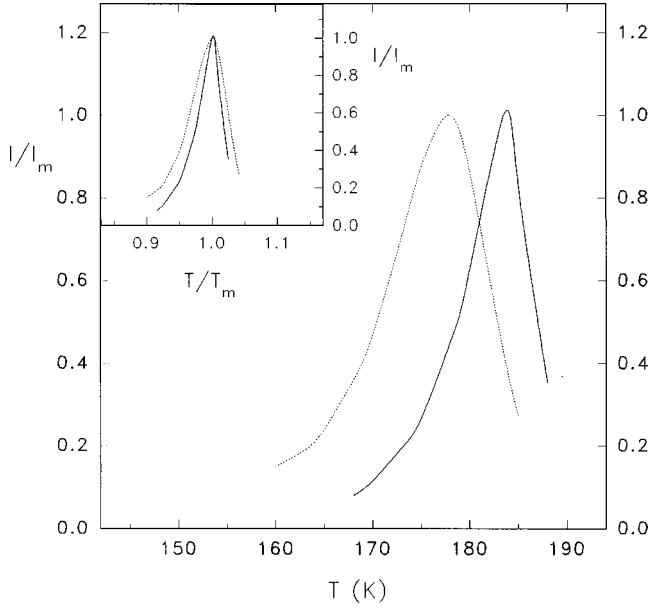


FIG. 5. TSDC thermograms normalized to unit height for NMEC bulk (—) and confined in BR,  $f=30\%$ , and  $d=7.6$  nm (---). The inset shows the corresponding scaling plots.

[Eq. (1)]. The shape of the dielectric loss function near a loss peak is characterized by two scaling parameters  $m$  and  $n$  ( $0 \leq m, n \leq 1$ ) related to the limiting behavior of the relaxation function<sup>25–27</sup>

$$\varepsilon''(\nu) \sim \nu^m \quad (\nu \ll \nu_0), \quad (4)$$

$$\varepsilon''(\nu) \sim \nu^{-n} \quad (\nu \gg \nu_0).$$

The parameters  $\alpha$  and  $\gamma$  in Eq. (1) are related to the scaling parameters by  $m=1-\alpha$  and  $n=(1-\alpha)\gamma$ . In Figs. 7 and 8

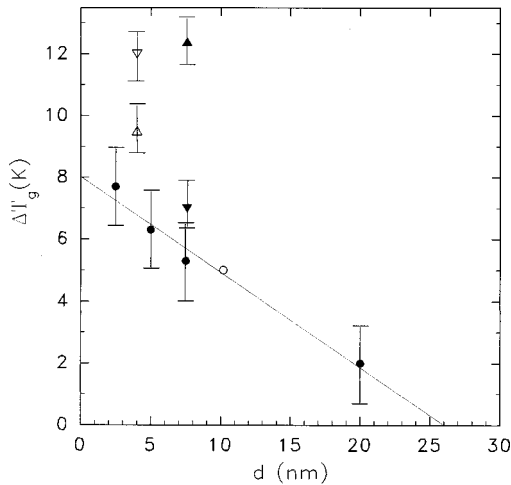


FIG. 6. Shift of glass transition temperature  $T_g$ ,  $\Delta T_g = T_g$  (bulk)  $- T_g$  (confined), vs nominal pore (droplet) diameter  $d$  for NMEC confined in different geometries: Gelsil, ●; Vioran (Ref. 1), ○; Vycor glass (TSDC), △; Vycor glass silanized (TSDC), ▽; BR, effective-medium corrected, ▲; BR (TSDC), ▽. The line is a guide for the eyes through the Gelsil data.

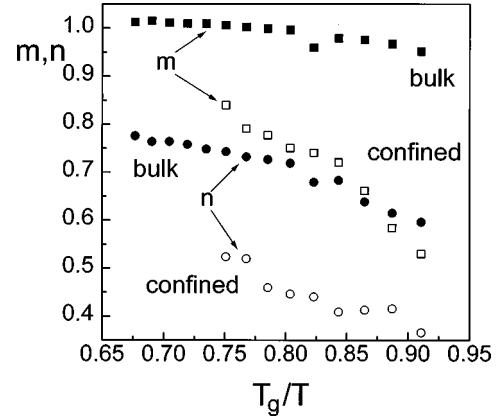


FIG. 7. Shape parameters  $m$  and  $n$  for the  $\alpha$  relaxation of NMEC bulk and confined in BR with  $f=30\%$  and  $d=7.6$  nm ( $m$  bulk, ■;  $n$  bulk, ●;  $m$  confined, □;  $n$  confined, ○).

we show the shape parameters  $m$  and  $n$  for NMEC confined in BR and in Gelsil glasses, respectively, against the scaled reciprocal temperature  $T_g/T$ .

#### IV. DISCUSSION

The assignment of the three relaxations in Figs. 1 and 2, Rel I and Rel II and  $\alpha$  process in the order of increasing frequency, to the interfacial liquid layer, the interfacial MWS polarization of the heterogeneous matrix-liquid system and the glass transition of the volume liquid, respectively, is in agreement with the results of Ref. 1. In that work the assignment was based on detailed MWS calculations and on measurements with chemically modified (silanized) and with partially filled CPG samples. In this work extensive MWS calculations of the relaxation strength and of the relaxation time of the theoretical interfacial loss peak using as input data the results of dielectric measurements on the pure com-

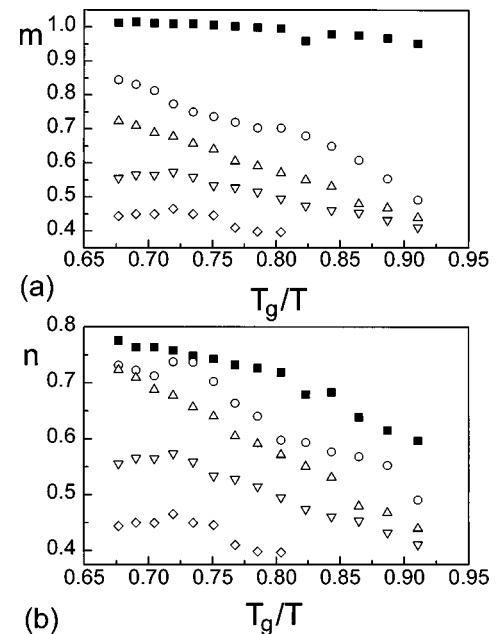


FIG. 8. Shape parameters  $m$  (a) and  $n$  (b) for the  $\alpha$  relaxation of NMEC bulk and confined in Gelsil glasses (bulk, ■; Gelsil 20 nm, ○; 7.5 nm, △; 5.0 nm, ▽; 2.5 nm, ◇).

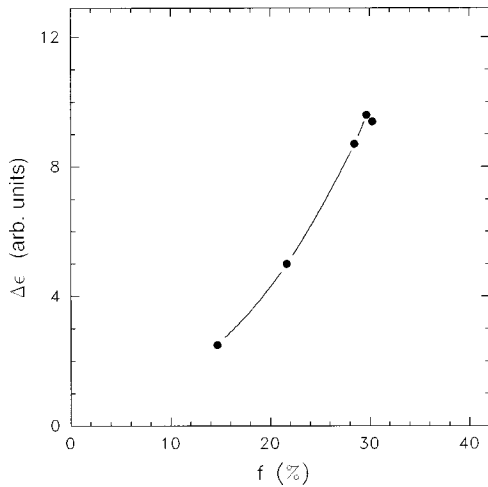


FIG. 9. Relaxation strength  $\Delta\epsilon$  of the  $\alpha$  relaxation obtained from TSDC measurements vs filling factor  $f$  for NMEC in BR.

ponents (i.e., confining matrix and bulk NMEC) (Ref. 21) give results similar to those measured for Rel II and, thus, provide additional support for that assignment. Moreover, the relaxation strength of Rel I, obtained by the fitting procedure described in the previous section and illustrated in Fig. 2, was found to drastically decrease with increasing temperature. This result is in agreement with Rel I being assigned to the interfacial liquid layer, if we consider that the thickness of that interfacial layer is expected to decrease with increasing temperature.

Figure 9 shows the dependence of the relaxation strength  $\Delta\epsilon$  of the TSDC peak associated with the glass transition (Fig. 4) on the filling factor  $f$  for NMEC in BR.  $\Delta\epsilon$ , in arbitrary units, is proportional to the normalized magnitude  $I_m$  of the TSDC peak (Fig. 4). From SAXS measurements we know that the mean droplet diameter  $d$  increases with increasing  $f$ .<sup>21</sup> We observe in Fig. 9 that, for high  $f$ ,  $\Delta\epsilon$  increases overlinearly with increasing  $f$ , in agreement with the assumption of the existence of a relatively immobile surface layer that does not contribute to the  $\alpha$  process in Figs. 1, 4, and 5.

It has already been mentioned in the previous section that conductivity effects at low frequencies are practically absent in the system BR-liquid (Fig. 1), whereas they are strong in the system CPG-liquid for both Gelsil (Fig. 1) and Vycor glasses. This is due to the fact that the liquid is confined in isolated droplets in BR and in interconnected pores (percolation) in CPG. A direct consequence is that the deconvolution of the complex broad low-frequency dispersion into two relaxations, Rel I and Rel II, is less straightforward for CPG compared to BR (Figs. 1 and 2). In fact, measurements on several glass-forming liquids confined in Gelsil glasses have been analyzed in terms of one or two relaxation processes in addition to the  $\alpha$  process.<sup>14,15</sup>

In the previous paragraphs we discussed our results in terms of the classification of the confined liquid into two fractions: an interfacial layer close to the walls and the volume liquid in the inner layers. The dynamics of both fractions is modified compared to the bulk liquid: the interfacial layer is relatively immobile, its relaxation being shifted by several decades to lower frequencies (Figs. 1 and 2); the relaxation of the volume liquid, on the contrary, becomes

faster compared to bulk as we will discuss further in this section. A two-state model with dynamic exchange between a bulklike phase in the pore volume and an interfacial phase close to the pore wall has been used to explain the results of DRS measurements on glass-forming liquids confined in Gelsil glasses.<sup>14</sup> An alternative interpretation in terms of a mesoscopically uniform but cooperative relaxation as stimulated by the theoretical work of Sappelt and Jäckle<sup>9</sup> has also been proposed.<sup>17</sup> In a recent paper Jérôme and Commandeur<sup>28</sup> combine both pure confinement and substrate effects in a picture of a uniform collective relaxation to interpret the results of second-harmonic generation measurements on the relaxation behavior of molecules of a glass-forming liquid crystal confined in a thin film on a silica plate.

The results in Fig. 3 show that the temperature dependence of the relaxation rate of the  $\alpha$  process in bulk NMEC and of the  $\alpha$  process and of Rel II [and probably also of Rel I (Ref. 1)] in NMEC in BR is described by the VFT equation (3). The same holds also for the dc conductivity in NMEC not shown in Fig. 3.<sup>21</sup> It is interesting to note that, while the relaxation rates for the  $\alpha$  process and for the MWS process (Rel II) are similar to those measured by Schüller, Richert, and Fischer<sup>1</sup> in NMEC confined in the pores of the CPG Bioran with  $d=10.2$  nm, the relaxation rates for the process assigned to the interfacial layer (Rel I in Fig. 3) are by about two decades larger in BR. Further, the relative magnitude of the relaxation strength of the interfacial layer process is larger in Bioran than in BR, these results suggesting stronger surface interactions in Bioran CPG than in BR. Thus, although very simple for the complex systems under investigation, the two-state model not only provides a consistent description of our experimental data, but allows the prediction of the behavior of the liquid in another confining matrix in agreement with existing experimental data.

Focusing now on the  $\alpha$  process, the relaxation rates are faster for the confined liquid compared to the bulk one. Similar results were obtained with the Gelsil glasses, the relaxation rates for the confined liquid decreasing with increasing pore diameter  $d$  towards those measured on the bulk liquid. These effects become weaker with increasing temperature/frequency. Correction of the values of the parameters which describe the behavior of the confined liquid following effective medium theories [Eq. (2)] provides only insignificant changes (Fig. 3 and Table I). Thus, the behavior of the confined liquid can in principle be discussed, at least for the high filling factors of our investigation, on the basis of the measured effective dielectric data.

In Fig. 6 we show all data available for the shift of the glass transition temperature  $\Delta T_g = T_g(\text{bulk}) - T_g(\text{confined})$  in NMEC confined in different geometries. In the case of DRS measurements  $T_g$  and  $\Delta T_g$  were obtained from extrapolations of the VFT fits (Fig. 3) to  $\tau=100$  s ( $\nu_0=1/628$  Hz). In the case of TSDC measurements  $\Delta T_g$  was taken as the shift of the peak temperature  $T_m$  (Figs. 4 and 5). We should mention in this connection that dielectric measurements are well suited for determining  $T_g$  values in close proximity to those obtained by the classical method of measuring  $T_g$ , namely, DSC; DRS and ac DSC measurements on the glass-forming liquid phenyl salicylate (salol) have shown that the corresponding Arrhenius plots practically coincide in the common frequency region of the two

techniques,<sup>29</sup> suggesting that both techniques probe at glass transition the mobility of units of similar size.

Some comments on the data shown in Fig. 6 are in order. Shifts of the same order of magnitude as  $\Delta T_g$  were obtained also for the Vogel temperature  $T_0$  in the VFT equation (2) from the DRS data (Table I) and, in principle,  $\Delta T_0$  could be considered as representative for the modifications of the glass transition dynamics induced by confinement, instead of  $\Delta T_g$ . The advantage of taking  $\Delta T_g$  is that TSDC data can be included (Fig. 6), as well as DSC data (work in progress). For NMEC in BR, for which we have  $\Delta T_g$  values determined by DRS and by TSDC on the same samples, there is some discrepancy between the two values ( $\Delta T_g = 7.5$  K by TSDC and  $\Delta T_g = 12.4$  K by DRS). This point deserves further experimental investigation. For the comparison BR-CPG it is interesting to note that for the same confining length  $d$  (pore diameter in CPG, droplet diameter in BR)  $\Delta T_g$  is larger in BR. We think that this difference reflects effects of the dimensionality of confinement (three dimensional in BR versus two dimensional in CPG). We will come back to this point later in discussing the effects of confinement on the shape of the response. DRS and TSDC measurements on the H-bonded liquid propylene glycol suggest strong effects of the dimensionality of confinement on  $\Delta T_g$ .<sup>48</sup> The detailed investigation of confinement effects on the glass transition of several H-bonded and nonassociating liquids in comparison to each other may reveal interesting aspects of the liquid dynamics and of the glass transition. For the quantitative comparison of different confining geometries with each other it should be kept in mind that the  $\alpha$  process in Fig. 6 refers to the inner mobile layer only, with the result that the relation to each other of the real sample sizes for different confining systems does not necessarily coincide with the relation to each other of the nominal confining lengths for the same systems. This might be the reason for the different behavior of the CPG Vycor compared to the CPG Gelsil in Fig. 6 [whereas the data on Vioran (Ref. 1) fit well with those on Gelsil].

The data on native and on silanized Vycor glass in Fig. 6, obtained as mean values from several measurements, clearly show that  $\Delta T_g$  is larger for the silanized sample. Two effects are induced by silanization: modification of the inner surface that becomes more hydrophobic and reduction of the confining length (the space left for the liquid).<sup>4,5</sup> The smaller the nominal confining length, the more important becomes the second effect. We inclined towards the explanation that the increase of  $\Delta T_g$  with silanization for NMEC in Vycor glass results from the reduction of the pore diameter, bearing in mind that practically no such effect was observed with the Bioran glasses with  $d = 10.2$  nm.<sup>1</sup> For a more quantitative explanation, comparative measurements on several silanized glasses combined with measurements of the reduced confining length would be needed.

Extrapolation of the straight line in Fig. 6 (a guide for the eyes through the Gelsil data) to  $\Delta T_g = 0$  gives a critical value  $d_c = 25$  nm. This allows the determination of the cooperativity length  $\xi$  as  $\xi \leq 12$ –13 nm (Fig. 10). Please note that the real sample size  $L$  is smaller than  $d$  due to the presence of the relatively immobile interfacial layer (Fig. 10), so that 12–13 nm is an upper limit for  $\xi$ . Values of  $\xi$  at  $T_g$  reported in the literature are a few nm.<sup>7,31</sup> The value of  $\xi$  determined here

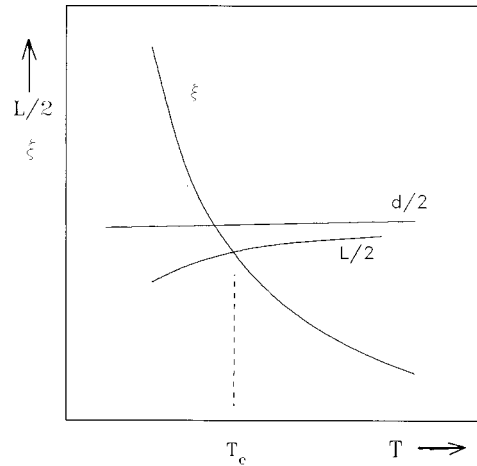


FIG. 10. Schematic diagram to illustrate the origin of confinement effects on the dynamics of the glass transition in glass-forming liquids. Confinement effects appear for  $L/2 < \xi$ . For a given  $d/2$  and  $L/2$  this occurs for  $T < T_c$ .

may appear as too large. We note, however, that positive  $\Delta T_g$  values were measured by DSC for several confined liquids, decreasing with increasing pore diameter  $d$  but still present at relatively large values of  $d$ .<sup>11</sup> In addition,  $\Delta T_g = 5$  K was measured for NMEC confined in 10.2-nm pores.<sup>1</sup> Following the same procedure as here,  $\xi \leq 5$ –6 nm was determined for the H-bonded liquid propylene glycol.<sup>48</sup>

The acceleration of the  $\alpha$  process, and as a direct consequence of that the lowering of  $T_g$ , of the confined liquid compared to the bulk one can be understood on the basis of the cooperativity concept in the configurational entropy model of glass formation of Adam and Gibbs;<sup>8</sup> see also Sec. I. This model explains the temperature dependence of relaxation phenomena in glass-forming liquids essentially in terms of the temperature dependence of the size  $\xi$  of the cooperatively rearranging region: the relaxation time  $\tau$  of this region increases with increasing  $\xi$ . If the size of the confined sample  $L$  (i.e., the thickness of the mobile inner layer/sphere in our experiments) is larger than  $2\xi$ , there is no size dependence in the dynamical behavior. On the other hand, if at a given temperature  $2\xi$  exceeds the size of the confined sample, all the molecules in the sample take part in the cooperative dynamics and the sample as a result will relax faster compared to bulk. Further, since  $\xi$  decreases towards zero with increasing temperature,<sup>6–8</sup> confinement effects weaken and finally disappear. Further, as the relaxation becomes faster in the confined liquid,  $T_g$  shifts to lower temperatures following the condition  $\tau(T_g) = 100$  s. The shift increases with decreasing confining length  $d$  (and sample size  $L$ ) (Fig. 10) and with increasing dimensionality of confinement. For quantitative estimations it should be taken into account that the real sample size  $L$  (i.e., the size of the mobile inner layer/sphere) increases with increasing temperature towards the nominal confining length  $d$ .<sup>4,5</sup> These relations are schematically illustrated in Fig. 10.

Using kinetic Ising and lattice-gas models with kinetic constraints as models of cooperative dynamics in undercooled liquids near the glass transition Sappelt and Jäckle concluded that confinement of glass-forming liquids in geometries of confining length comparable to the cooperativity

length  $\xi$  should lead to retardation of the  $\alpha$  process and to an increase of the glass transition temperature  $T_g$ .<sup>9</sup> The reason for that is that with the confining length decreasing below  $\xi$ , an increasing number of molecules are permanently blocked and no longer contribute to the response of the system to external perturbations.<sup>9</sup> Monte Carlo simulations by Ray and Binder<sup>30</sup> of the dynamics near the glass transition in a two-dimensional lattice model of polymer melt, on the other hand, show that, at low temperatures, the diffusion constant increases with decreasing size of the sample. According to the authors, these results suggest the possibility of the existence of cooperatively rearranging regions,<sup>8</sup> whose mean size increase as the temperature is lowered. The lowering of  $T_g$  for the confined liquid observed in our measurements is in agreement with theoretical predictions by Hunt<sup>18</sup> and in disagreement with the results of molecular-dynamics simulations for one dimensionally confined glass-forming liquid that predict an increase of  $T_g$ .<sup>19</sup>

In the theoretical models and computer simulations mentioned above it is always assumed that the confined liquid is the same as the bulk one (e.g., with respect to the density). This point, which is experimentally very difficult to prove, forms a basic assumption in the interpretation of our data as in other similar studies.<sup>1,10,11–17</sup> On the other hand, shifts of  $T_g$  to lower temperatures for liquids confined in CPG's have been assigned to reduction of the density of the confined liquid compared to that of the bulk liquid,<sup>11</sup> a point for which there is, however, no experimental evidence. In addition, due to the counter pressure of the elastic rubber matrix, a reduction of the density is less probable for our three dimensionally confined droplets.

It is interesting to compare our results on 2D and 3D confined liquids with those obtained with 1D confined polymers.<sup>32–38</sup> Several experimental techniques have been used to measure glass transition properties of thin polymeric films, typically supported on a substrate. Depending on film thickness and on substrate shifts of  $T_g$  to both lower<sup>32,34,36,38</sup> and higher<sup>32,33</sup> temperatures have been measured. Confinement effects, polymer-substrate interactions, and the presence of a free surface (as well as density reduction in the film<sup>34</sup>) were used to explain the observed changes of  $T_g$ . In Ref. 36 a three-layer model, incorporating a dead layer near the substrate, a surface layer with reduced  $T_g$ , and a bulklike layer between these interfaces, has been used to explain the results. It has also been suggested that a region with an elevated  $T_g$  exists near the polymer-substrate interface.<sup>38</sup> Measurements on freely standing polystyrene films, however, show that, compared to bulk,  $T_g$  decreases linearly with decreasing film thickness.<sup>35</sup> Schick and Donth<sup>39</sup> and Laredo *et al.*<sup>40</sup> measured the glass transition properties of specially prepared semicrystalline polymer samples in the hope of detecting confinement effects on the amorphous phase. Whereas no  $T_g$  shift was observed in polyethylene terephthalate, where the amorphous phase forms films,<sup>39</sup> a shift of  $T_g$  to lower temperatures, compared to the bulk, was observed in polycarbonate and related to speculations on the organization of the mobile amorphous phase in droplets.<sup>40</sup>

Interesting effects of confinement were observed on the collective dynamics of the isotropic-nematic phase transition of liquid crystal confined in CPG.<sup>41,42</sup> The transition shifts to lower temperatures, the transition region becomes broader,

and the bulk nematic phase is replaced by a “glassy” state.<sup>41</sup> Measurements in the bulk pretransitional region show a drastic decrease of the relaxation time compared to the bulk.<sup>42</sup>

In the following we discuss the changes induced by confinement on the width and the shape of the  $\alpha$  process (Figs. 7 and 8). In agreement with the results of measurements on confined liquids,<sup>1,10–15</sup> confined polymers,<sup>37</sup> and confined liquid crystals,<sup>41,42</sup> confinement induces a broadening of the response observed in both DRS (Fig. 1) and TSDC measurements (Figs. 4 and 5). This broadening may be linked to increased local scale heterogeneity,<sup>37</sup> in analogy to the broadening of the  $\alpha$ -relaxation distribution in bulk glass-forming liquids and polymers as temperature is decreased towards  $T_g$  having been linked to increased heterogeneity caused by local density fluctuations.<sup>43</sup> In DRS measurements the shape of the response is quantitatively described by the scaling parameters  $m$  and  $n$ , the slopes at frequencies lower and higher than the loss peak frequency, respectively, in log-log plots [Eq. (4)]. We observe in Figs. 7 and 8 that for NMEC bulk  $m$  is approximately 1 over the whole temperature range ( $m \geq 0.95$ , decreasing with decreasing temperature) and  $n < 1$  ( $0.6 < n < 0.8$ ), decreasing with decreasing temperature. In NMEC confined in BR (Fig. 7) both  $m$  and  $n$  are clearly smaller than 1 (broadening of the response), decreasing with decreasing temperature. The  $T$  dependence of  $n$  is rather small and it is interesting to note that  $n$  takes values lower than 0.5.<sup>44</sup> The asymmetry of the loss peak for the bulk liquid ( $m > n$ ) is observed also for the confined liquid.

For NMEC confined in Gelsil the asymmetry parameter  $\gamma$  in the Havriliak-Negami equation (1) is, within the limits of accuracy, equal to 1 for the pore diameters studied, with the result that  $m = n$  (Fig. 8).  $m$  and  $n$  decrease with decreasing temperature and, for the same temperature, with decreasing pore diameter. Comparison of Figs. 7 and 8 with each other shows that for the same confining length  $d$  (7.6 nm in BR, 7.5 nm in Gelsil) the response is broader in BR, suggesting stronger effects for three- than two-dimensional confinement. Interestingly, the  $m$  values are similar in BR and in Gelsil, whereas  $n$  is smaller in BR. The change from asymmetric response in BR (and in bulk) to a symmetric one in Gelsil was observed also with the H-bonded propylene glycol.<sup>48</sup>

We would like to stress that it is difficult to attribute the broadening of the response for the  $\alpha$  process of the confined liquid to inner surface interactions, as there is strong experimental evidence that the  $\alpha$  process analyzed here refers to the inner mobile layer only (two-state model). In addition, if we assume a reduction of the density of the confined liquid compared to the bulk density as the origin of the lowering of  $T_g$  of the confined liquid,<sup>11</sup> a narrowing rather than a broadening of the response for the  $\alpha$  process of the confined liquid should be expected, in agreement with the results of dielectric measurements in glass-forming glycerol as a function of pressure.<sup>45</sup>

With respect to the changes induced in the shape of the response the behavior of NMEC (and of propylene glycol) in Gelsil resembles that of semicrystalline polymers.<sup>46</sup> We can only speculate at this stage that the similarity may arise from similar constraints upon the amorphous phase imposed by the crystallites in the semicrystalline samples and the rigid porous matrix in the CPG. We note also that the values of  $m$  are more or less similar to each other in BR and in CPG,



whereas those of  $n$  are clearly lower in BR than in CPG, for the same confining length. In terms of models proposed for the interpretation of  $m$  and  $n$  and for the prediction of the relaxational behavior of materials,<sup>25,26</sup> these results imply increased correlation of short-range (local) motions in BR compared to CPG, which might be linked to the dimensionality of confinement.

## V. CONCLUSIONS

Summarizing, we have studied in detail confinement effects on the dynamics of the glass transition of N-methyl- $\epsilon$ -caprolactam, as a representative of nonassociating low-molecular-weight glass-forming liquids, by means of dielectric techniques. In addition to CPG, used in very recent years by several investigators in confinement studies, where the liquid is two dimensionally confined in the system of interconnected pores, we used BR with hydrophilic inclusions, where the liquid is three dimensionally confined in droplets. We paid special attention in controlled variation of the experimental conditions (matrix material, size of confinement, dimensionality of confinement, condition of inner surfaces) in an attempt to separate pure confinement from other effects. The basic assumption there is that true confinement effects are present in all these experiments, whereas other effects may sensitively depend on the specific experimental conditions.

The results suggest the existence of two fractions of liquid in the confined geometry: a relatively immobile interfacial layer close to the wall and the volume liquid in the inner layers. The dynamics of the interfacial layer is mainly determined by liquid-wall interactions that give rise to a slow relaxation process, whereas the volume liquid experiences pure confinement effects. Thus, in a sense, chemical effects are separated from physical effects. Although very simple,

the model allows predictions verified by experiments on other systems.<sup>1</sup>

The  $\alpha$  relaxation associated with the glass transition of the confined volume liquid is faster compared to the bulk liquid. As a result of that the glass transition temperature  $T_g$  is lower for the confined volume liquid compared to the bulk one. The shift of  $T_g$ ,  $\Delta T_g = T_g(\text{bulk}) - T_g(\text{confined})$ , increases with decreasing pore diameter  $d$  and is larger for three- than for two-dimensional confinement. These results can be understood on the basis of the configurational entropy model of Adam and Gibbs. In terms of the cooperatively rearranging regions and the cooperativity length  $\xi$ , size effects on the glass transition appear as soon as  $\xi$ , increasing with decreasing temperature, becomes larger than  $d$ . The results allow to determine  $\xi$  at  $T_g$  to  $\xi \leq 10-12$  nm.

Confinement induces a broadening of the  $\alpha$  relaxation, which may be linked with increased local scale heterogeneity. The broadening is larger for three- than for two-dimensional confinement and increases with decreasing  $d$ . The asymmetric shape of the  $\alpha$  response of the bulk liquid is observed also for NMEC confined in BR, whereas the response is symmetric for NMEC confined in CPG. The behavior of the liquid in CPG resembles that of semicrystalline polymers.

Measurements on propylene glycol, as a representative of H-bonded liquids, confined in the same geometries, show results similar in many aspects to those described here.<sup>48</sup> Studies on more liquids, selected on the basis of the degree of H bonding, on the size and the shape of the molecule and the fragility index<sup>47</sup> are in progress and critical discussion on their comparative results may shed more light on the phenomenon of glass transition. Bearing in mind the complexity of the systems under investigation, experiments that could provide information on possible changes of the structure of the liquid induced by confinement would be of significant importance.

<sup>1</sup>J. Schüller, R. Richert, and E. W. Fischer, *Phys. Rev. B* **52**, 15 232 (1995).

<sup>2</sup>J. van Turnhout, in *Electrets*, edited by G. M. Sessler (Springer, Berlin, 1980), p. 81.

<sup>3</sup>P. Pissis, A. Ananagstopoulou-Konsta, L. Apekis, D. Daoukaki-Diamanti, and C. Christodoulides, *J. Non-Cryst. Solids* **131-133**, 1174 (1991).

<sup>4</sup>*Dynamics in Small Confining Systems*, edited by J. M. Drake, J. Klafter, R. Kopelmann, and D. D. Awschalom, MRS Symposia Proceedings No. 290 (Materials Research Society, Pittsburgh, 1993).

<sup>5</sup>*Dynamics in Small Confining Systems II*, edited by J. M. Drake, J. Klafter, R. Kopelmann, and S. M. Troian, MRS Symposia Proceedings No. 366 (Materials Research Society, Pittsburgh, 1995).

<sup>6</sup>J. Jäckle, *Rep. Prog. Phys.* **49**, 171 (1986).

<sup>7</sup>E. Donth, *Relaxation and Thermodynamics in Polymers. Glass Transition* (Akademie Verlag, Berlin, 1992).

<sup>8</sup>G. Adam and J. H. Gibbs, *J. Chem. Phys.* **43**, 139 (1965).

<sup>9</sup>D. Sappelt and J. Jäckle, *J. Phys. A* **26**, 7325 (1993).

<sup>10</sup>P. Pissis, D. Daoukaki-Diamanti, L. Apekis, and C. Christodoulides, *J. Phys.: Condens. Matter* **6**, L325 (1994).

<sup>11</sup>C. L. Jackson and G. B. McKenna, *J. Non-Cryst. Solids* **131-133**, 221 (1991).

<sup>12</sup>J. Zhang, G. Liu, and J. Jonas, *J. Phys. Chem.* **96**, 3478 (1992).

<sup>13</sup>J. Schüller, Yu. B. Mel'nichenko, R. Richert, and E. W. Fischer, *Phys. Rev. Lett.* **73**, 2224 (1994).

<sup>14</sup>M. Arndt, R. Stannarius, W. Gorbatschow, and F. Kremer, *Phys. Rev. E* **54**, 5377 (1996).

<sup>15</sup>W. Gorbatschow, M. Arndt, R. Stannarius, and F. Kremer, *Europhys. Lett.* **35**, 719 (1996).

<sup>16</sup>C. Streck, Yu. B. Mel'nichenko, and R. Richert, *Phys. Rev. B* **53**, 5341 (1996).

<sup>17</sup>R. Richert, *Phys. Rev. B* **54**, 15 762 (1996).

<sup>18</sup>A. Hunt, *Solid State Commun.* **90**, 527 (1994).

<sup>19</sup>T. Fehr and H. Löwen, *Phys. Rev. E* **52**, 4016 (1995).

<sup>20</sup>R. Pelster, A. Kops, G. Nimtz, A. Enders, H. Kretzmann, P. Pissis, A. Kyritsis, and D. Woermann, *Ber. Bunsenges. Phys. Chem.* **97**, 666 (1993).

<sup>21</sup>G. Barut, Ph.D. thesis, University of Cologne, Germany, 1996.

<sup>22</sup>R. Pelster, *IEEE Trans. Microwave Theory Tech.* **43**, 1494 (1995).

<sup>23</sup>C. J. F. Böttcher and P. Bordewijk, *Theory of Electric Polarization*, 2nd ed. (Elsevier, Amsterdam, 1978), Vol. II, p. 72.

- <sup>24</sup>L. K. H. van Beek, in *Progress in Dielectrics*, edited by J. B. Birks (Heywood, London, 1967), Vol. 7.
- <sup>25</sup>L. A. Dissado and R. M. Hill, Proc. R. Soc. London, Ser. A **390**, 131 (1983).
- <sup>26</sup>A. Schönhals and E. Schlosser, Colloid Polym. Sci. **267**, 125 (1989).
- <sup>27</sup>A. K. Jonscher, *Dielectric Relaxation in Solids* (Chelsea Dielectrics, London, 1983).
- <sup>28</sup>B. Jérôme and J. Commandeur, Nature (London) **386**, 589 (1997).
- <sup>29</sup>P. K. Dixon, Phys. Rev. B **42**, 8179 (1990).
- <sup>30</sup>P. Ray and K. Binder, Europhys. Lett. **27**, 53 (1994).
- <sup>31</sup>E. W. Fischer, E. Donth, and W. Steffen, Phys. Rev. Lett. **68**, 2344 (1992).
- <sup>32</sup>J. L. Keddie, R. A. L. Jones, and R. A. Gory, Faraday Discuss. **98**, 219 (1994); Europhys. Lett. **27**, 59 (1994).
- <sup>33</sup>J. H. van Zanten, W. E. Wallace, and W.-L. Wu, Phys. Rev. E **53**, R2053 (1996).
- <sup>34</sup>G. Reiter, Europhys. Lett. **23**, 579 (1993).
- <sup>35</sup>J. A. Forrest, K. Dalnoki-Veress, J. R. Stevens, and J. R. Dutcher, Phys. Rev. Lett. **77**, 2002 (1996).
- <sup>36</sup>G. B. DeMaggio, W. E. Frieze, and D. W. Gidley, Phys. Rev. Lett. **78**, 1524 (1997).
- <sup>37</sup>D. B. Hall, J. C. Hooker, and J. M. Torkelson, Macromolecules **30**, 667 (1997).
- <sup>38</sup>O. Brucker, S. Christian, H. Bock, C. W. Frank, and W. Knoll, Polym. Prepr. (Am. Chem. Soc. Div. Polym. Chem.) **88**, 918 (1997).
- <sup>39</sup>C. Schick and E. J. Donth, Phys. Scr. **43**, 423 (1991).
- <sup>40</sup>E. Laredo, M. Grimaud, A. Müller, A. Bello, and N. Suarez, J. Polym. Sci., Part B: Polym. Phys. **34**, 2863 (1996).
- <sup>41</sup>X. I. Wu, W. I. Goldberg, M. X. Liu, and J. Z. Xue, Phys. Rev. Lett. **69**, 470 (1992).
- <sup>42</sup>G. Schwalb and F. W. Deeg, Phys. Rev. Lett. **74**, 1383 (1995).
- <sup>43</sup>K. L. Ngai and D. Plazek, Rubber Chem. Technol. **68**, 376 (1995).
- <sup>44</sup>A. Schönhals, F. Kremer, and E. Schlosser, Phys. Rev. Lett. **67**, 999 (1991).
- <sup>45</sup>M. Paluch, S. J. Rzoska, P. Habdas, and J. Ziolo, J. Phys.: Condens. Matter **8**, 10 885 (1996).
- <sup>46</sup>Y. Ishida, K. Yamafuji, H. Ito, and M. Takayanagi, Kolloid Z. Z. Polym. **184**, 97 (1962).
- <sup>47</sup>C. A. Angell, J. Non-Cryst. Solids **131–133**, 13 (1991).
- <sup>48</sup>P. Pissis, A. Kyritsis, D. Daoukaki, G. Barut, R. Pelster, and G. Nimitz, J. Phys.: Condens. Matter (to be published).